The Dynamics of Star Polymers in Fast Extensional Flow and Stress Relaxation

Qian Huang[1], Serena Agostini[2], Ludovica Hengeller[1], Maksim Shivokhin[3], Nicolas J. Alvarez[4], Lian R. Hutchings[2], and Ole Hassager[1]

[1] *Department of Chemical and Biochemical Engineering, Technical University of Denmark, Lyngby, Denmark*
[2] *Durham Centre for Soft Matter, Department of Chemistry, Durham University, Durham, United Kingdom*
[3] *Department of Chemical and Biological Engineering and Center for Molecular Study of Condensed Soft Matter, Illinois Institute of Technology, Chicago, United States*
[4] *Department of Chemical and Biological Engineering, Drexel University, Philadelphia, United States*

(Dated: Aug. 01, 2016)

Abstract

In the present work, we confirm the observation from Ianniruberto and Marrucci [1] that entangled melts of branched polystyrenes behave like linear polystyrenes in the steady state of fast extensional flow, by measuring a linear, an asymmetric star and a symmetric star polystyrenes with the same span molecular weight (180 kg/mol). We show that all three melts reach the same extensional steady-state viscosity in fast extensional flow (faster than the inverse Rouse time). We further measure stress relaxation following steady extensional flow for the three melts. We show that initially they relax in a similar way, most likely via arm retraction, at short time, but behave differently at long time due to both the length of the arm and the branch point. The terminal relaxation is described by a Doi and Edwards based model, i.e. considering pure orientational relaxation.

1 Introduction

It is well known that the rheological behavior of polymers is intimately related to their molecular structure. The tube model, which is the most prolific theory proposed by Doi, Edwards, and de Gennes [2, 3], has been modified for more than three decades and has successfully predicted the linear viscoelastic (LVE) properties of entangled polymer systems with different molecular structures (e.g. [4, 5, 6, 7]). But the tube model poorly describes polymer dynamics in nonlinear flows, especially in extensional flow. Recent experimental and theoretical works on linear polymer chains suggest that the inclusion of anisotropic molecular friction in the tube model could increase the agreement between model predictions and experimental trends[8, 9, 10, 11, 12, 13, 14].

However, industrial polymers are not always linear polymers. For example, low-density polyethylenes (LDPEs) are long-chain branched polymers. Although theoretical predictions of the nonlinear rheology for LDPEs have shown some success [15, 16], the models are quantitatively weak in predicting experimental observations at large deformation in fast extensional flow [17, 18]. The underlying mechanism governing the nonlinear response of branched polymers is still unclear due to the lack of experimental data and for the case of LDPE due to its complex random branched structure. Starting with a well-defined branched structure is paramount in understanding the contribution of branches to nonlinear extensional flow. Recently, Ianniruberto and Marrucci [1] reported that entangled melts of branched polystyrenes (PS) behave like linear PS in the steady state of fast extensional flow. This interesting conclusion is based on the data from Nielsen et al. [19] for a star and a pompom PS, which is, to our knowledge, the only published data of steady-state viscosity in strong extensional flow for branched polymers of well-defined structures.

In this work, we systematically explore the nonlinear dynamics of model branched polymers starting from the simplest structure, which are star polymers with three arms. We investigated three PS melts, a symmetric star, an asymmetric star and a linear PS, in both fast extensional flow and stress relaxation. We show that the three melts behave identically in the steady state of fast extensional flow, which is in

agreement with the observation from Ianniruberto and Marrucci [1]. However, in stress relaxation following steady extensional flow, relaxation of the different samples depends on the presence of the branch point and the length of the arm.

2 Experimental

2.1 Materials

Three PS melts with different molecular structures, a linear PS Lin180, an asymmetric star PS Star20, and a symmetric star PS Star90, were synthesized via anionic polymerization. All three PS molecules have the same backbone of molecular weight 180kg/mol, and an arm located in the center of the backbone of molecular weight 0kg/mol(Lin180), 20kg/mol(Star20) and 90kg/mol(Star90), respectively. The molecular structures are illustrated in Figure 1.

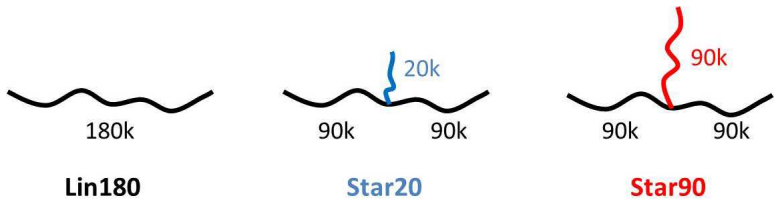

Figure 1: Illustration of molecular structures for Lin180, Star20 and Star90.

The details of synthesis for Star20 and Star90 can be found in Ref. [20]. Table 1 summarizes the weight average molecular weight M_w and the polydispersity index Đ for the two star polymers, where the values are taken from Table 4 in Ref. [20]. PS lin180 was synthesized by living anionic polymerization under high vacuum conditions by using sec-BuLi as initiator and the reaction was carried out in benzene overnight and terminated with nitrogen-sparged methanol. The sample was then further purified by fractionation in toluene/methanol to remove high molecular weight impurities formed during termination. The size exclusion chromatography (SEC) analysis has been carried out as reported in Ref. [20] for the stars, and the values are also listed in Table 1.

Table 1: The properties of the polystyrenes

Sample name	Molar mass of long arm		Molar mass of short arm		Molar mass of polymer	
	M_w[g/mol]	Đ	M_w[g/mol]	Đ	M_w[g/mol]	Đ
Lin180	–	–	–	–	187000	1.02
Star20	92400	1.03	20500	1.05	208300	1.03
Star90	92400	1.03	–	–	289100	1.03

2.2 Mechanical spectroscopy

The LVE properties of the PS were obtained from small amplitude oscillatory shear (SAOS) measurements. An 8mm parallel plate geometry was used on an ARES–G2 rheometer from TA instruments. The measurements were performed at different temperatures between 130 °C and 160 °C under nitrogen. For each sample, the data was shifted to a single master curve at the reference temperature $T_r = 130\,^{\circ}\mathrm{C}$ using the time–temperature superposition (TTS) procedure. As shown in the inset of Figure 2(a), the temperature shift factor a_T for all the PS samples was found to follow the Williams-Landel-Ferry (WLF) equation

$$\log_{10} a_T = \frac{-c_1^0 (T - T_r)}{c_2^0 + (T - T_r)}, \tag{1}$$

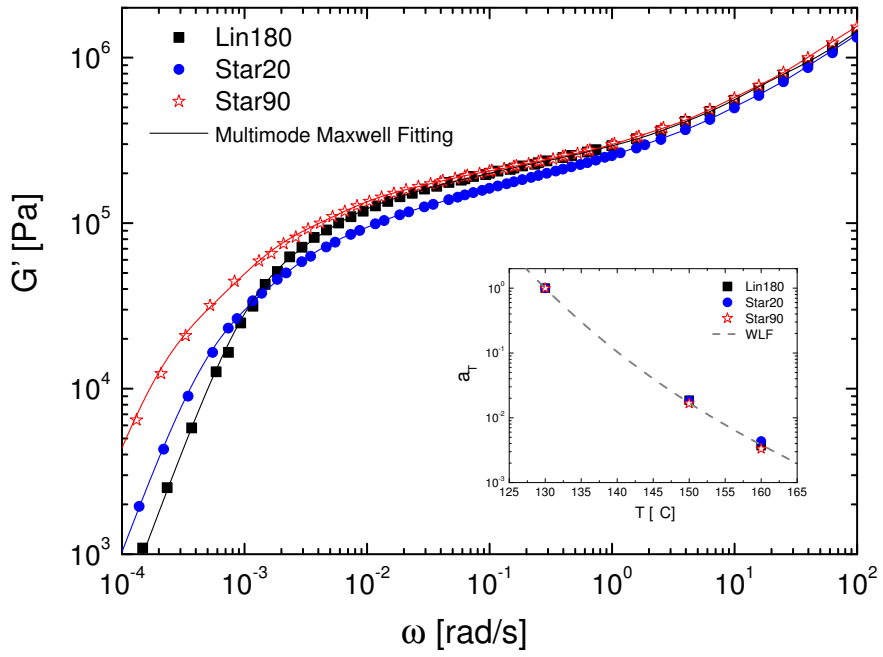

(a)

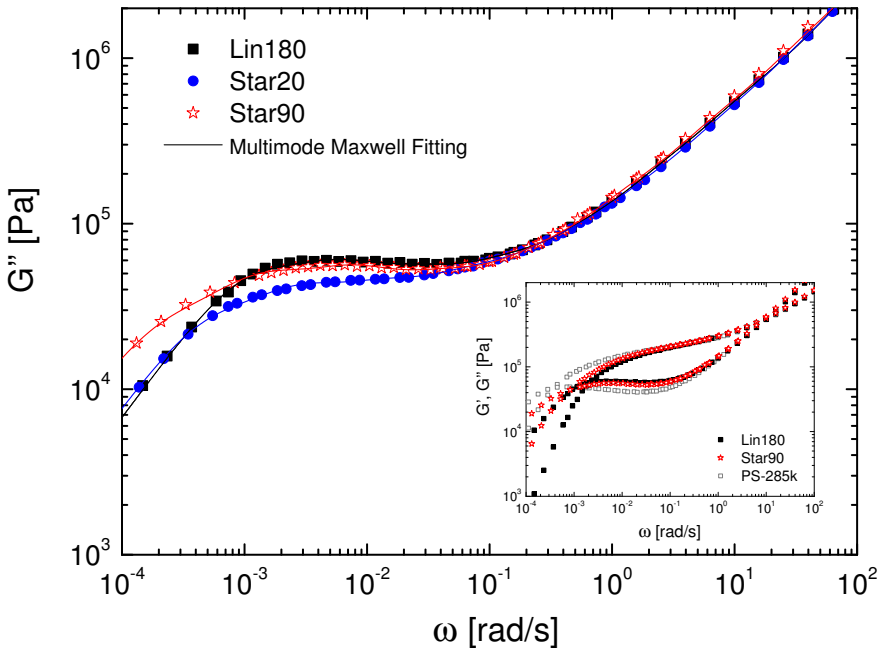

(b)

Figure 2: LVE data fitted with the multimode Maxwell spectrum at 130 °C for Lin180, Star20 and Star90. (a) Storage modulus G' as a function of angular frequency ω; The inset shows the temperature shift factor a_T for the three samples. (b) Loss modulus G'' as a function of angular frequency ω; The inset shows both G' and G'' for Lin180, Star90 and PS-285k. The data of PS-285k is taken from Ref.[10].

where $c_1^0 = 8.99$, $c_2^0 = 81.53$K, $T_r = 130\,^\circ$C, and T is temperature in $^\circ$C [21]. Figure 2 shows the storage modulus G' and loss modulus G'' as a function of angular frequency ω for all the samples. At high frequency (approximately $\omega > 1$ rad/s), the G', G'' data almost overlap each other, indicating the three PS samples have similar glass transition temperatures. The LVE behavior for well entangled polymer systems is characterized by the entanglement density. To be specific, for nearly monodisperse linear polymers, it is characterized by the number of entanglements per chain Z. In our previous work, we have shown that linear polymer melts and solutions with the same Z have the same normalized shape of G', G'' curves [10, 12, 13]. Since each linear polymer chain has two ends, Z can be also understood as the number of entanglements per two chain-ends. If we define Z_e as the number of entanglements per chain-end, then Lin180 and Star90 have the same Z_e. From Figure 2, it can be seen that the G', G'' curves of Lin180 and Star90 overlap each other over a wide frequency range in the viscoelastic regime where $G' > G''$ (see the inset of Figure 2(b)). This is essentially in accordance with the fact that a symmetric star polymer with arm mass M_a and a tethered chain of mass M_a have the same Rouse time [1]. By contrast, the G', G'' curves of Star90 in the viscoelastic regime do not overlap with the linear PS-285k (data taken from Ref. [10]) which has the same molecular weight, due to the fact that PS-285k has a larger Z_e. The G', G'' curves of Lin180 and Star90 differ in the flow regime at low frequency (approximately $\omega < 0.002$ rad/s) due to the branch point. As for the asymmetric star PS, the short arm of Star20 is not well entangled (about one entanglement) and thus relax much faster than the backbone. In the viscoelastic regime, Star20 shows lower G', G'' values than Star90 and Lin180, indicating the relaxed arms behave like a solvent which dilutes the system. In the flow regime, Star20 shows higher G', G'' values than Lin180, also due to the existence of the branch point.

2.3 Extensional stress measurements

The extensional stress was measured by a filament stretching rheometer (FSR) [22]. Prior to making a measurement, the samples were molded into cylindrical test specimens with a fixed radius of $R_0 = 2.7$mm. The initial length L_0 of the test specimens was controlled by the addition of a given mass of the sample into the mold. The aspect ratio $\Lambda_0 = L_0/R_0$ is between 0.46 and 0.60. The samples were pressed at 150 $^\circ$C and annealed at the same temperature under vacuum until the polymer chains were completely relaxed.

All the samples were pre–stretched to a radius R_p ranging from 1.1mm to 1.8mm at 150 $^\circ$C prior to the experiments. After pre–stretching, the temperature was decreased to 130 $^\circ$C for the extensional stress measurements. The samples were kept under a nitrogen environment during all measurements. They were checked by SEC again after the extensional stress measurements to ensure that there was no degradation.

During the extensional measurements, the force $F(t)$ is measured by a load cell and the diameter $2R(t)$ at the mid-filament plane is measured by a laser micrometer. At small deformation in the startup of the elongational flow, part of the stress difference comes from the radial variation due to the shear components in the deformation field. This effect may be compensated by a correction factor as described in Ref. [23]. The Hencky strain and the mean value of the stress difference over the mid–filament plane are then calculated as

$$\epsilon\left(t\right) = -2\ln\left(R\left(t\right)/R_p\right) \tag{2}$$

and

$$\left\langle \sigma_{zz} - \sigma_{rr} \right\rangle = \frac{F\left(t\right) - m_f g/2}{\pi R(t)^2} \cdot \frac{1}{1 + \left(R\left(t\right)/R_0\right)^{10/3} \cdot \exp\left(-\Lambda_0^3\right)/\left(3\Lambda_0^2\right)}, \tag{3}$$

where m_f is the weight of the filament and g is the gravitational acceleration. The strain rate is defined as $\dot{\epsilon} = d\epsilon/dt$. A recently updated control scheme [24] is employed in the FSR to ensure accurate constant strain rate. The extensional stress growth coefficient is defined as $\bar{\eta}^+ = \left\langle \sigma_{zz} - \sigma_{rr} \right\rangle/\dot{\epsilon}$. In the stress relaxation phase following the startup of uniaxial extension, the mid-diameter of the filament is kept constant by the control scheme, giving $\dot{\epsilon} = 0$. The extensional stress decay coefficient is defined as $\bar{\eta}^- = \left\langle \sigma_{zz} - \sigma_{rr} \right\rangle/\dot{\epsilon}$, where $\dot{\epsilon}$ is the strain rate in the startup of the flow.

3 Results and Discussion

3.1 Startup and steady–state extensional flow

Figure 3(a) shows the extensional stress growth coefficient as a function of time at different strain rates for the three PS melts. The measurements of the lowest strain rate ($0.0003s^{-1}$) were originally performed at 150 °C and shifted to 130 °C using the TTS procedure. All the other measurements were performed at 130 °C directly. The LVE envelope in the figure is calculated by

$$\bar{\eta}^+(t) = 3\sum g_i\tau_i(1 - e^{-t/\tau_i}), \tag{4}$$

where g_i and τ_i are obtained by fitting the LVE data in Figure 2 with the 10-mode Maxwell relaxation spectrum. The 10-mode Maxwell relaxation modulus $G(t)$ is given by

$$G(t) = \sum_{i=1}^{10} g_i e^{-t/\tau_i}. \tag{5}$$

The values of g_i and τ_i are listed in Table 2.

Table 2: Linear viscoelastic spectrum for the PS melts at 130 °C

Sample	Lin180		Star20		Star90	
	τ_i[s]	g_i[Pa]	τ_i[s]	g_i[Pa]	τ_i[s]	g_i[Pa]
	0.00068	$3.076 \cdot 10^7$	0.00068	$3.076 \cdot 10^7$	0.00068	$3.076 \cdot 10^7$
	0.00322	$1.479 \cdot 10^6$	0.00322	$1.479 \cdot 10^6$	0.00322	$1.479 \cdot 10^6$
	0.01525	$5.347 \cdot 10^5$	0.02201	$6.251 \cdot 10^5$	0.02144	$7.509 \cdot 10^5$
Relaxation	0.07226	$3.660 \cdot 10^5$	0.11062	$2.446 \cdot 10^5$	0.12209	$2.817 \cdot 10^5$
spectrum	0.34231	$1.328 \cdot 10^5$	0.55594	$1.042 \cdot 10^5$	0.69525	$1.112 \cdot 10^5$
	1.62159	$6.097 \cdot 10^4$	2.79398	$6.049 \cdot 10^4$	3.95906	$5.451 \cdot 10^4$
	7.68170	$5.108 \cdot 10^4$	14.0417	$4.929 \cdot 10^4$	22.5447	$4.840 \cdot 10^4$
	36.3893	$4.872 \cdot 10^4$	70.5689	$4.408 \cdot 10^4$	128.380	$6.682 \cdot 10^4$
	172.381	$6.852 \cdot 10^4$	354.657	$5.126 \cdot 10^4$	731.056	$6.451 \cdot 10^4$
	816.595	$6.577 \cdot 10^4$	1782.40	$3.135 \cdot 10^4$	4162.97	$2.725 \cdot 10^4$

It can be seen that at low stretch rates, the three melts behave differently in extensional flow, which is consistent with their different LVE envelope. However, in the fast extensional flow (i.e. at strain rates faster than $0.003s^{-1}$), the melts with different molecular structures interestingly behave identically. They show the same extensional stress growth coefficient in the startup of the flow, and reach the same steady-state viscosity. It is more clear to see the identical behavior of the three melts in Figure 4(a), where the extensional steady-state viscosity is plotted as a function of the stretch rate. By contrast, with the same molecular weight, PS-285k (data taken from Ref.[10]) is more strain hardening than Star90 and reaches higher steady-state viscosity values at the same stretch rates, as shown in Figure 3(b). This difference is attributed to the different Rouse time. The Rouse time for PS-285k is about 203s at 130 °C [10], while for Star90 is about 87s (the same as Lin180). If we plot the steady stress (normalized by the plateau modulus, G_N^0 = 250kPa for all the PS samples) as a function of the Weissenberg number $Wi_R = \dot{\epsilon}\tau_R$ (assuming Star20 also has the same Rouse time as Lin180 and Star90), a master curve is obtained at $Wi_R > 1$ which scales with ${Wi_R}^{0.5}$, as shown in Figure 4(b). This observation agrees with the suggestion by Ianniruberto and Marrucci (Figure 6 in Ref.[1]) that entangled melts of branched PS (stars and pompoms) behave like linear PS in the steady state of fast elongational flow.

3.2 Stress relaxation following extensional flow

As mentioned above, in fast extensional flow ($Wi_R > 1$), the data suggests that the effects caused by the presence of the arm and the branch point are shielded. Both asymmetric Star20, causing dilution in LVE, and the symmetric Star90 behave identically with the linear PS Lin180. We now ask whether the three polymers have the same behavior in stress relaxation, especially at short time scales. To investigate this

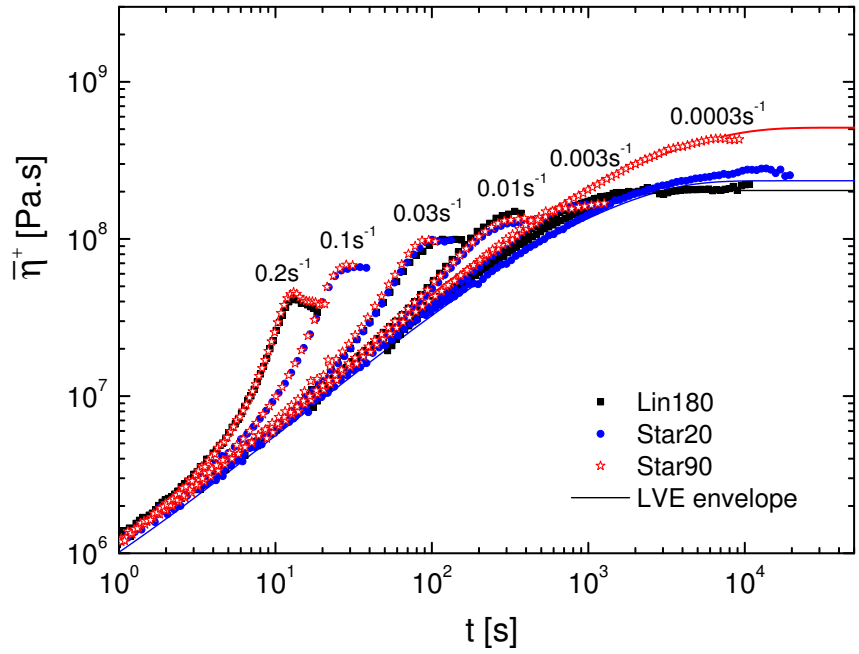

(a)

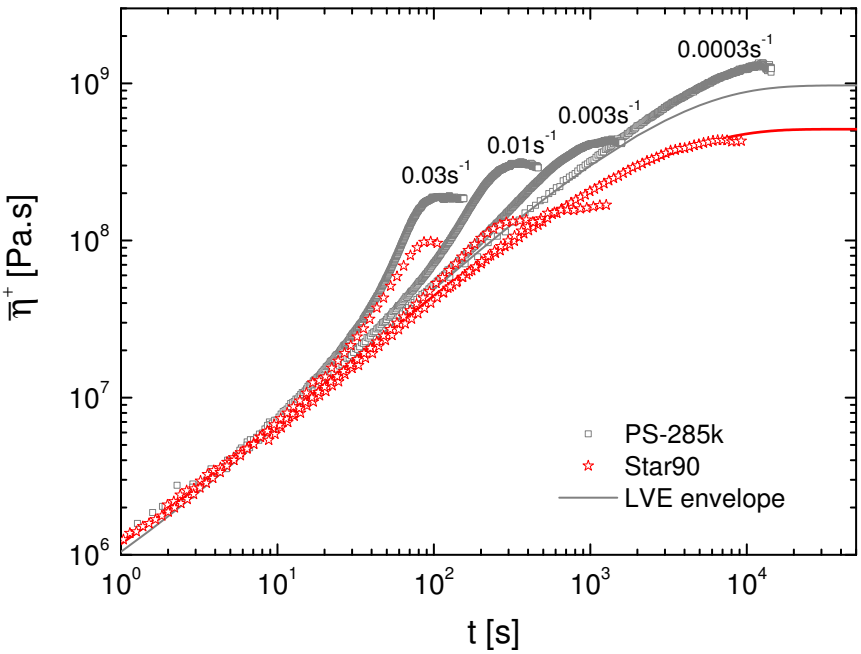

(b)

Figure 3: The measured extensional stress growth coefficient as a function of time at different strain rate at 130 °C for (a) Lin180, Star20 and Star90; (b) Star90 and PS-285k. Data of PS-285k is taken from Ref.[10].

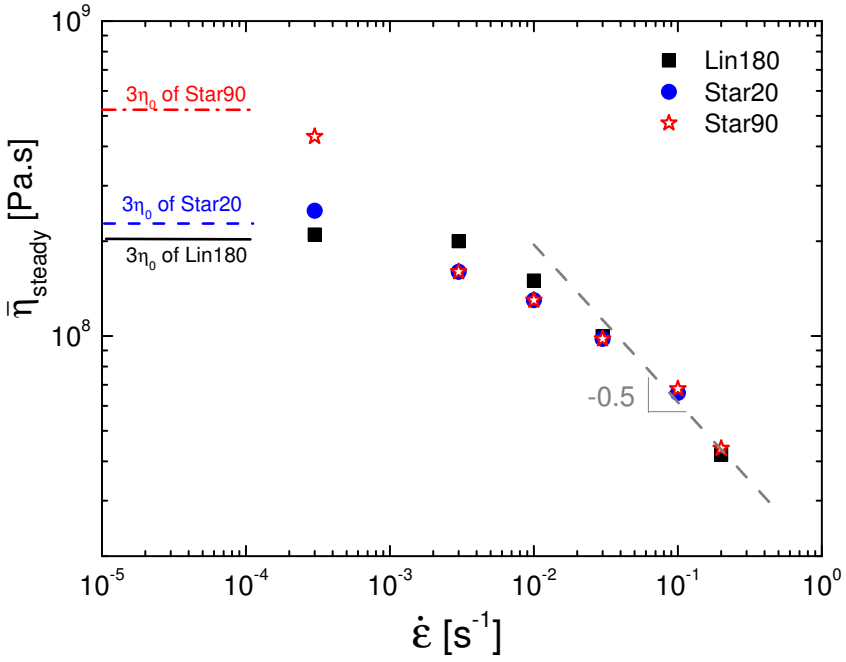

(a)

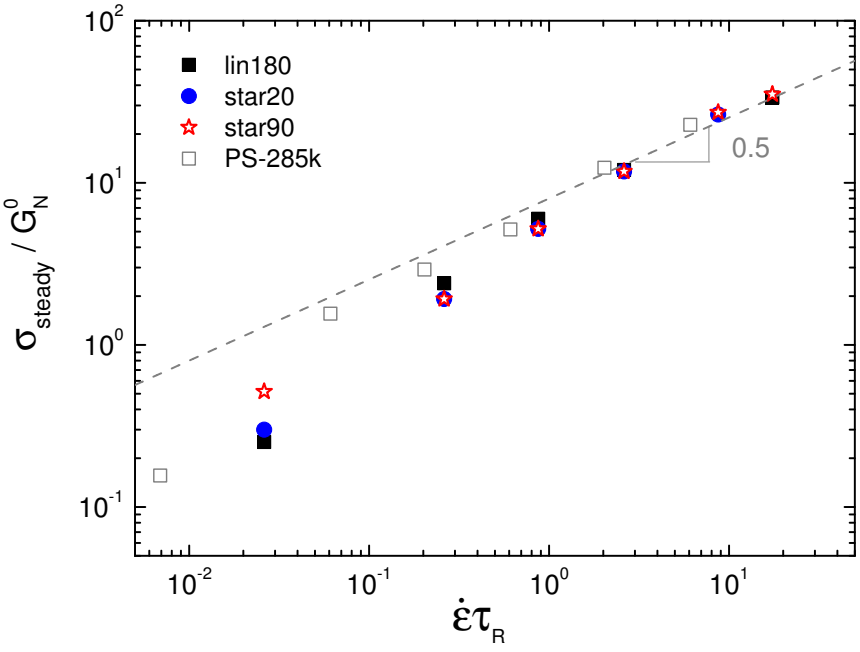

(b)

Figure 4: (a) The extensional steady-state viscosity as a function of strain rate for Lin180, Star20 and Star90 at 130 °C.(b) The normalized steady stress as a function of Weissenberg number for all the melts. Data of PS-285k is taken from Ref.[10].

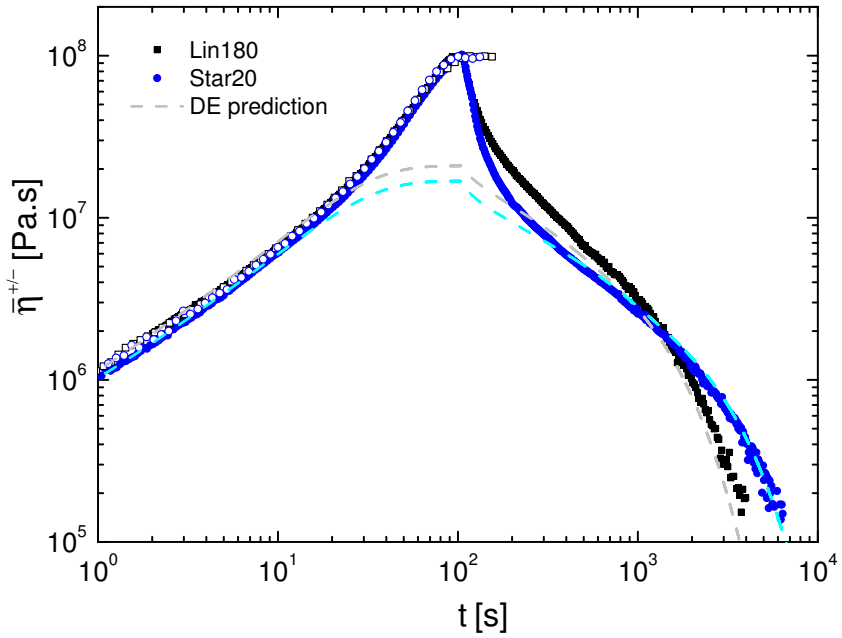

(a)

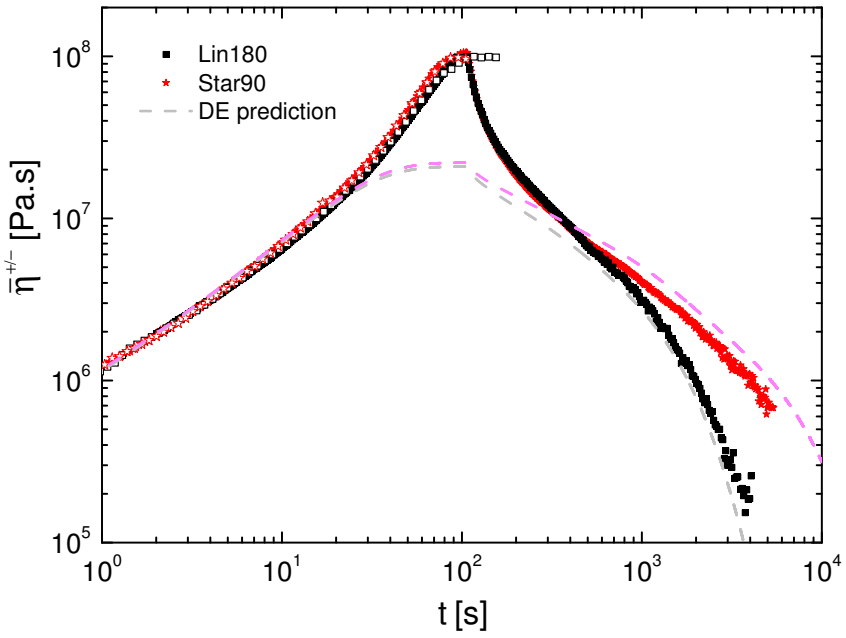

(b)

Figure 5: The measured extensional stress growth/decay coefficient as a function of time at 130 °C for (a) Lin180 and Star20; (b) Lin180 and Star90. For each measurement, the startup of the flow is uniaxial extension with constant strain rate $0.03s^{-1}$. The flow is stopped and followed by stress relaxation at Hencky strain 3.2. The open symbols are the corresponding data of uniaxial extension taken from Figure 3.

question, each melt was stretched with the constant strain rate 0.03s^{-1} at 130 °C, which is faster than the inverse Rouse time $1/\tau_R$ (about 0.01s^{-1}), until reaching steady state at Hencky strain 3.2 where the flow was stopped and the stress decay coefficient was measured. When steady state is reached, the relaxation behavior is unaffected by the imposed Hencky strain [25]. Therefore it is not necessary to stop the flow at a Hencky strain value higher than 3.2.

Figure 5 shows the results. Each measurement in the figure was repeated at least once to confirm reproducibility. In the stress relaxation regime shown in Figure 5(a), Star20 initially overlaps Lin180 at short time. After which, Star20 relaxes faster than Lin180, showing a lower stress decay coefficient. This faster relaxation of Star20 is most likely due to the relaxed short arm, which behaves like a solvent and acts to dilute the backbone. At longer times, Star20 relaxes slower than Lin180, which is indicated by the fact that the Star20 relaxation curve crosses Star90, leading to a quantitatively larger stress decay coefficient. As mentioned in the LVE discussion, the slower relaxation at long time is most likely due to the branch point of Star20. In comparison, the relaxation of Star90 and Lin180 are quantitatively similar for much longer time, as shown in Figure 5(b). However at long time very similar to Star20, Star90 relaxes slower than Lin180 , which again is argued to be due to the branch point.

As a reference for the nonlinear behavior, we first compare the data with the prediction of the original reptation based model introduced by Doi and Edwards [2]. The stress tensor of the Doi–Edwards (DE) model is expressed as

$$\boldsymbol{\sigma}(t) = \int_{-\infty}^{t} M(t-t')\mathbf{S}_{\text{DE}}(t,t')\text{d}t'. \tag{6}$$

The original DE model utilizes a specific form of the LVE memory function $M(t-t')$ developed for monodisperse linear polymers. This form from the original DE model will not fit the LVE properties of the star polymers. Since we focus on the nonlinear properties in extensional flow, here for LVE properties we just use the multi-mode Maxwell memory function

$$M(t-t') = \sum\nolimits_i \frac{g_i}{\tau_i} e^{-(t-t')/\tau_i}, \tag{7}$$

which corresponds to the experimentally determined relaxation function with parameters g_i and τ_i in table 2. $\mathbf{S}_{\text{DE}}$ in Eq.6 is the strain tensor given by

$$\mathbf{S}_{\text{DE}}(t,t') = \frac{15}{4}\frac{1}{\langle|\mathbf{E}\cdot\mathbf{u}|\rangle}\left\langle\frac{\mathbf{E}\cdot\mathbf{u}\;\mathbf{E}\cdot\mathbf{u}}{|\mathbf{E}\cdot\mathbf{u}|}\right\rangle, \tag{8}$$

where $\mathbf{u}$ is the unit vector and $\mathbf{E}$ is the relative deformation gradient tensor. The bracket denotes an average over an isotropic distribution. A K–BKZ representation that closely approximates the rigorous DE model has been provided by Hassager and Hansen [26].

The dashed lines in Figure 5 show the results of the DE prediction. Since Eq.6 does not include the evolution of chain stretch, the predicted results do not capture the strain hardening behavior in the startup of the flow and thus reach a much lower steady-state value. However, in the relaxation regime, the DE model predicts reasonably well the relaxation behavior of both linear and star PS at long time.

We further analyze the results by re-plotting and scaling the data of the relaxation in Figure 5. We shift the time $t = 0$ to the time when relaxation starts, and normalize the stress decay coefficient by the value at $t = 0$ (when relaxation starts). The plots are shown in Figure 6(a). Three regions are identified in the figure. At very short time in Region I (approximately <15s), the relaxation of the three melts are identical. At intermediate times, Region II (approximately between 15s and 500s), Star90 and Lin180 still behave identically, while Star20 relaxes faster. At long times, Region III (approximately >500s), the relaxation of all three melts are different from each other. As mentioned above, the relaxation behavior in Region III is well described by the DE model. Regarding Region I and II, if we assume the arms relax independently and simultaneously, and also assume Lin180 as a two-arm star, it is not surprising that three relaxation curves overlap. These arguments also explain the relaxation behavior of Star20. In Region I Star20 relaxes very similar (e.g. via arm retraction) as Star90 and Lin180. In Region II, the short arm of Star20 is completely relaxed, resulting in a lower stress level for the diluted system. However, if we vertically shift the relaxation curve of Star20 up, the curve of Star20 in Region II overlaps that of Star90 as shown in Figure 6(b). This strongly suggests that the remaining two arms of Star20 relax via the same mechanisms as Star90 and Lin180.

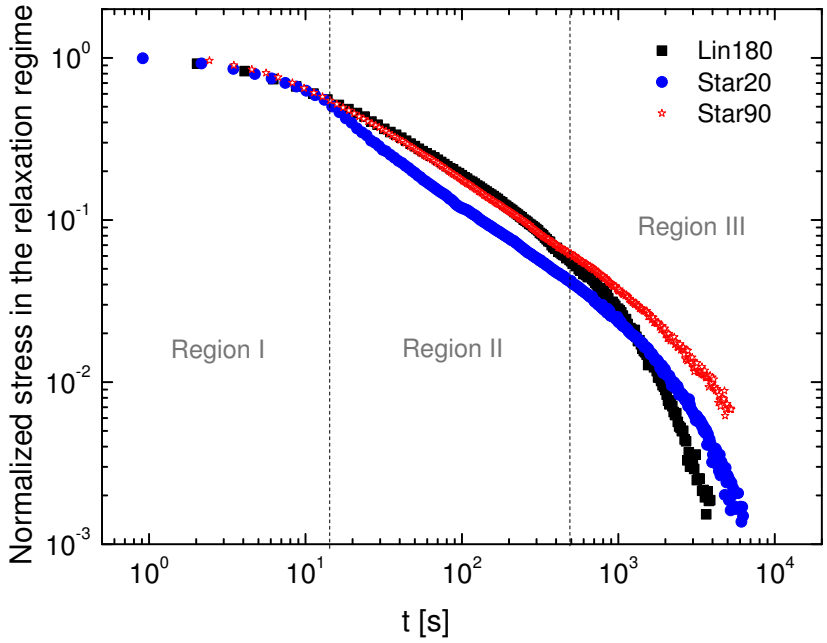

(a)

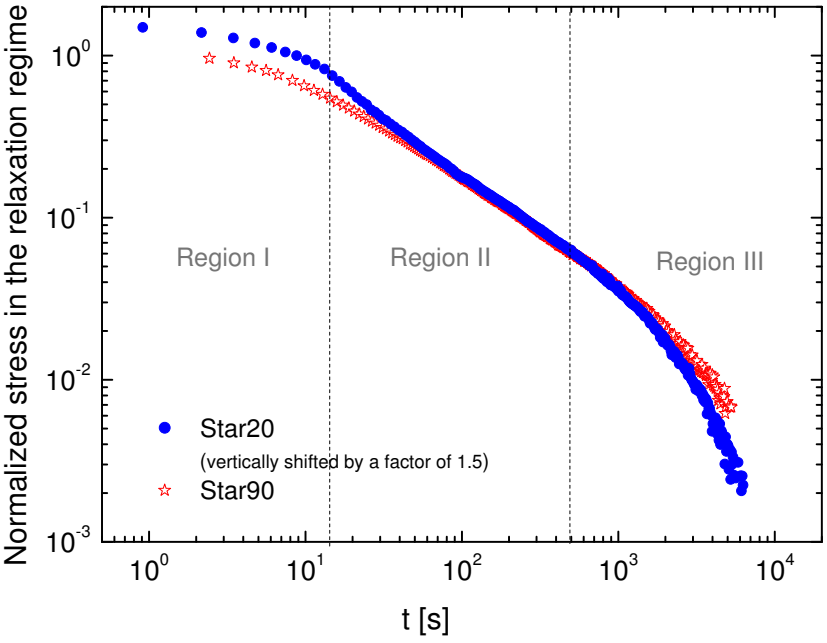

(b)

Figure 6: The normalized stress decay coefficient as a function of time at 130 °C for (a) Lin180, Star20 and Star90. The data are taken from the stress relaxation phase from Figure 5. The time $t = 0$ is shifted to the time when relaxation starts, and the stress decay coefficient is normalized by the value when relaxation starts. (b) Star20 and Star90; The data of Star20 is vertically shifted up with a factor of 1.5.

4 Conclusions

We have shown that linear (Lin180), asymmetric star (Star20) and symmetric star (Star90) PS melts with the same molecular weight backbone reach the same extensional steady-state viscosity in fast extensional flow (faster than the inverse Rouse time) at the same Weissenberg number based on the backbone Rouse time. The effects from the arm and the branch point appear to be shielded causing all PS melts to behave like linear PS, as previously suggested by Ianniruberto and Marrucci [1]. We further explored the dynamics in stress relaxation following steady extensional flow. The relaxation at long time (terminal relaxation) is well described by a Doi and Edwards based model, i.e. considering pure orientational relaxation (via arm length fluctuation and reptation). At short time, the analysis of the relaxation data suggests that all three melts relax similarly via arm retraction. More work, e.g. characterization by neutron scattering on quenched PS samples, are necessary for a full understanding of the nonlinear dynamics of branched polymers.

Acknowledgement

QH and OH would like to acknowledge financial support from the Aage og Johanne Louis–Hansen Foundation. QH, SA, MS, LRH and OH would like to acknowledge financial support from the European Union Seventh Framework Programme [FP7/2007–2013] under grant no.214627–DYNACOP. LH and OH would like to acknowledge financial support from the Danish Council for Independent Research - Natural Sciences under grant no. 0602-02179B –EPMEF. NJA and OH would like to acknowledge financial support from the Danish Council for Independent Research - Technology and Production Sciences under grant no. 10-082409.

References

[1] Ianniruberto, G.; Marrucci, G. Entangled Melts of Branched PS Behave Like Linear PS in the Steady State of Fast Elongational Flows. Macromolecules 2013, 46, 267–275.

[2] Doi, M.; Edwards, S. F. The Theory of Polymer Dynamics. Clarendon Press: Oxford, U.K., 1986.

[3] de Gennes, P. G. Reptation of a Polymer Chain in the Presence of Fixed Obstacles. J. Chem. Phys. 1971, 55, 572–579.

[4] Milner, S. T.; McLeish, T. C. B. Parameter-Free Theory for Stress Relaxation in Star Polymer Melts. Macromolecules 1997, 30, 2159–2166.

[5] McLeish, T. C. B.; Allgaier, J.; Bick, D. K.; Bishko, G.; Biswas, P.; Blackwell, R.; Blottiere, B.; Clarke, N.; Gibbs, B.; Groves, D. J.; Hakiki, A.; Heenan, R. K.; Johnson, J. M.; Kant, R.; Read, D. J.; Young, R. N. Dynamics of Entangled H-Polymers:âĂŤ Theory, Rheology, and Neutron-Scattering. Macromolecules 1999, 32, 6734–6758.

[6] Larson, R. G. Combinatorial Rheology of Branched Polymer Melts. Macromolecules 2001, 34, 4556–4571.

[7] Lee, J. H.; Fetters, L. J.; Archer, L. A. Stress Relaxation of Branched Polymers. Macromolecules 2005, 38, 10763–10771.

[8] Ianniruberto, G.; Brasiello, A.; Marrucci, G. Simulations of Fast Shear Flows of PS Oligomers Confirm Monomeric Friction Reduction in Fast Elongational Flows of Monodisperse PS Melts As Indicated by Rheooptical Data. Macromolecules 2012, 45, 8058–8066.

[9] Yaoita, T.; Isaki, T.; Masubuchi, Y.; Watanabe, H.; Ianniruberto, G.; Marrucci, G. Primitive Chain Network Simulation of Elongational Flows of Entangled Linear Chains: Stretch/Orientation-induced Reduction of Monomeric Friction. Macromolecules 2012, 45, 2773–2782.

[10] Huang, Q.; Mednova, O; Rasmussen, H. K.; Alvarez, N. J.; Skov, A. L.; Almdal, K.; Hassager, O. Concentrated Polymer Solutions are Different from Melts: Role of Entanglement Molecular Weight. Macromolecules 2013, 46, 5026–5035.

[11] Huang, Q.; Alvarez, N. J.; Matsumiya„Y.; Rasmussen, H. K.; Watanabe, H.; Hassager, O. Extensional Rheology of Entangled Polystyrene Solutions Suggests Importance of Nematic Interactions. ACS Macro Lett. 2013, 2, 741–744.

[12] Huang, Q.; Hengeller, L; Alvarez, N. J.; Hassager, O. Bridging the Gap between Polymer Melts and Solutions in Extensional Rheology. Macromolecules 2015, 48, 4158–4163.

[13] Wingstrand, S. L.; Alvarez, N. J.; Huang, Q.; Hassager, O. Linear and Nonlinear Universality in the Rheology of Polymer Melts and Solutions. Phys. Rev. Lett. 2015, 115, 078302.

[14] Ianniruberto, G. Extensional Flows of Solutions of Entangled Polymers Confirm Reduction of Friction Coefficient. Macromolecules 2015, 48, 6306–6312.

[15] Read, D. J.; Auhl, D.; Das, C.; den Doelder, J.; Kapnistos, M.; Vittorias, I.; McLeish, T. C. B. Linking Models of Polymerization and Dynamics to Predict Branched Polymer Structure and Flow. Science 2011, 333, 1871–1874.

[16] Huang, Q.; Mangnus, M.; Alvarez, N. J.; Koopmans, R.; Hassager, O. A New Look at Extensional Rheology of Low-density Polyethylene. Rheol. Acta 2016, 55, 343–350.

[17] Rasmussen, H. K.; Nielsen, J. K.; Bach, A.; Hassager, O. Viscosity Overshoot in the Start-up of Uniaxial Elongation of Low Density Polyethylene Melts. J. Rheol. 2005, 49, 369–381.

[18] Huang, Q.; Rasmussen, H. K.; Skov, A. L.; Hassager, O. Stress Relaxation and Reversed Flow of Low-density Polyethylene Melts Following Uniaxial Extension. J. Rheol. 2012, 56, 1535–1554.

[19] Nielsen, J. K.; Rasmussen, H. K.; Denberg, M.; Almdal, K.; Hassager, O. Nonlinear Branch-Point Dynamics of Multiarm Polystyrene. Macromolecules 2006, 39, 8844–8853.

[20] Agostini, S.; Hutchings, L. R. Synthesis and Temperature Gradient Interaction Chromatography of Model Asymmetric Star Polymers by the "Macromonomer" Approach. European Polymer Journal 2013, 49, 2769–2784.

[21] Huang, Q. Molecular Rheology of Complex Fluids. Ph.D. thesis, Technical University of Denmark, 2013

[22] Bach, A.; Rasmussen, H. K.; Hassager, O. Extensional Viscosity for Polymer Melts Measured in the Filament Stretching Rheometer. J. Rheol. 2003, 47, 429–441.

[23] Rasmussen, H. K.; Bejenariu, A. G.; Hassager, O.; Auhl, D. Experimental Evaluation of the Pure Configurational Stress Assumption in the Flow Dynamics of Entangled Polymer Melts. J. Rheol. 2010, 54, 1325–1336.

[24] Román Marín, J. M.; Huusom, J. K.; Alvarez, N. J.; Huang, Q.; Rasmussen, H. K.; Bach, A.; Skov, A. L.; Hassager, O. A Control Scheme for Filament Stretching Rheometers with Application to Polymer Melts. J. Non-Newtonian Fluid Mech. 2013, 194, 14–22.

[25] Hengeller, L.; Huang, Q.; Dorokhin, A.; Alvarez, N. J.; Almdal, K.; Hassager, O. Stress Relaxation of Bi-disperse Polystyrene Melts. Rheol. Acta 2016, 55, 303–314.

[26] Hassager, O., Hansen, R. Constitutive Equations for the DoiâĂŞEdwards Model Without Independent Alignment. Rheol. Acta 2010, 49, 555–562.

For Table of Contents use only

The Dynamics of Star Polymers in Fast Extensional Flow and Stress Relaxation

Qian Huang, Serena Agostini, Ludovica Hengeller, Maksim Shivokhin, Nicolas J. Alvarez, Lian R. Hutchings, and Ole Hassager